NASA/TM-2004-213507

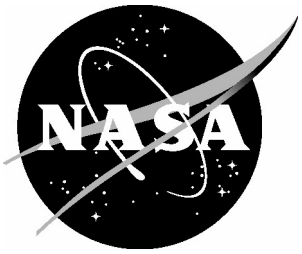

A Water Vapor Differential Absorption LIDAR Design for Unpiloted Aerial Vehicles

Patricia F. Mead
Norfolk State University, Norfolk, Virginia

Russell J. DeYoung
Langley Research Center, Hampton, Virginia

December 2004

The NASA STI Program Office . . . in Profile

Since its founding, NASA has been dedicated to the advancement of aeronautics and space science. The NASA Scientific and Technical Information (STI) Program Office plays a key part in helping NASA maintain this important role.

The NASA STI Program Office is operated by Langley Research Center, the lead center for NASA's scientific and technical information. The NASA STI Program Office provides access to the NASA STI Database, the largest collection of aeronautical and space science STI in the world. The Program Office is also NASA's institutional mechanism for disseminating the results of its research and development activities. These results are published by NASA in the NASA STI Report Series, which includes the following report types:

- TECHNICAL PUBLICATION. Reports of completed research or a major significant phase of research that present the results of NASA programs and include extensive data or theoretical analysis. Includes compilations of significant scientific and technical data and information deemed to be of continuing reference value. NASA counterpart of peer-reviewed formal professional papers, but having less stringent limitations on manuscript length and extent of graphic presentations.

- TECHNICAL MEMORANDUM. Scientific and technical findings that are preliminary or of specialized interest, e.g., quick release reports, working papers, and bibliographies that contain minimal annotation. Does not contain extensive analysis.

- CONTRACTOR REPORT. Scientific and technical findings by NASA-sponsored contractors and grantees.

- CONFERENCE PUBLICATION. Collected papers from scientific and technical conferences, symposia, seminars, or other meetings sponsored or co-sponsored by NASA.

- SPECIAL PUBLICATION. Scientific, technical, or historical information from NASA programs, projects, and missions, often concerned with subjects having substantial public interest.

- TECHNICAL TRANSLATION. English-language translations of foreign scientific and technical material pertinent to NASA's mission.

Specialized services that complement the STI Program Office's diverse offerings include creating custom thesauri, building customized databases, organizing and publishing research results ... even providing videos.

For more information about the NASA STI Program Office, see the following:

- Access the NASA STI Program Home Page at ***http://www.sti.nasa.gov***

- E-mail your question via the Internet to help@sti.nasa.gov

- Fax your question to the NASA STI Help Desk at (301) 621-0134

- Phone the NASA STI Help Desk at (301) 621-0390

- Write to:
  NASA STI Help Desk
  NASA Center for AeroSpace Information
  7121 Standard Drive
  Hanover, MD 21076-1320

NASA/TM-2004-213507

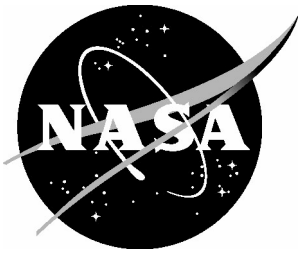

A Water Vapor Differential Absorption LIDAR Design for Unpiloted Aerial Vehicles

Patricia F. Mead
Norfolk State University, Norfolk, Virginia

Russell J. DeYoung
Langley Research Center, Hampton, Virginia

National Aeronautics and
Space Administration

Langley Research Center
Hampton, Virginia 23681-2199

December 2004

Available from:

NASA Center for AeroSpace Information (CASI)
7121 Standard Drive
Hanover, MD 21076-1320
(301) 621-0390

National Technical Information Service (NTIS)
5285 Port Royal Road
Springfield, VA 22161-2171
(703) 605-6000

A Water Vapor Differential Absorption LIDAR Design for Unpiloted Aerial Vehicles

Patricia F. Mead
Optical Engineering Department, Norfolk State University, Norfolk, VA 23504

Russell J. DeYoung
Langley Research Center, Hampton, VA 23681

Abstract

This system study proposes the deployment of a water vapor Differential Absorption LIDAR (DIAL) system on an Altair unmanned aerial vehicle (UAV) platform. The Altair offers improved payload weight and volume performance, and longer total flight time as compared to other commercial UAV's. This study has generated a preliminary design for an Altair based water vapor DIAL system. The design includes a proposed DIAL schematic, a review of mechanical challenges such as temperature and humidity stresses on UAV deployed DIAL systems, an assessment of the available capacity for additional instrumentation (based on the proposed design), and an overview of possible weight and volume improvements associated with the use of customized electronic and computer hardware, and through the integration of advanced fiber-optic and laser products. The results of the study show that less than 17% of the available weight, less than 19% of the volume capacity, and approximately 11% of the electrical capacity is utilized by the proposed water vapor DIAL system on the Altair UAV.

1. Introduction

Light Detection and Ranging (LIDAR), a technique that was adapted from its radio frequency analog, RADAR, is currently used at NASA Langley to execute a wide range of research investigations in atmospheric science. For example, NASA Langley has deployed ground and airborne LIDAR systems to characterize water vapor, ozone, and aerosols in our atmosphere. This report presents a system study of a water vapor Differential Absorption LIDAR (DIAL) system that would be implemented on an unmanned aerial vehicle (UAV) platform.

LIDAR sensors have been used since the 1960's to study the earth's atmosphere. These early LIDAR systems were initially ground-based platforms, and demonstrated the ability of these instruments to aid researchers to better understand surface topography, global energy transactions, weather and climatology systems and models, or other environmental characteristics of the atmosphere.

Early lidar systems were controlled in ground-based stations that required human operators to adjust and monitor the instruments. The limited range of laser sources and the limited available computing power also challenged lidar. Many important technological advances have helped to eliminate these challenges. In particular, the development of small, compact laser sources, an increased variety of laser sources, the

development of fiber optic devices, and the miniaturization of electronic components. Other important advances include the availability of newer, lighter materials and the emergence of wireless networks that can be linked into our global positioning infrastructure. It is now possible to initiate designs for compact LIDAR systems that might be deployed from space-borne platforms.

Atmospheric water vapor resides primarily in the troposphere, and although its concentration ranges from 10^{14} molecules/cm^3 at 12,000 km to 10^{18} molecules/cm^3 at ground level [Jursa, 1985], it plays a critical role in a variety of atmospheric processes, including climate, energy transfer, and the transfer of pollutants. Water vapor is a primary agent in cloud formation and the development of violent storms. Through its role in condensation and evaporation, water vapor acts as a stabilizing agent; preventing excessive temperature swings over short periods of time. The latent heat characteristics of water vapor are a primary agent in the development of hurricanes, and researchers hope to create accurate climate models through a better understanding of the role that water vapor plays in weather. Real time measurements of global water vapor would substantially improve weather prediction capabilities.

UAV's are an emerging tool in atmospheric science. Their use in military reconnaissance and battlefield oversight has been well documented due to the success of the Predator UAV in recent conflicts around the world [Parker, 2002]. As early as 1985, NASA has been involved in the development of UAV-based missions for non-military applications. In 1999, NASA's Environmental Research and Sensor Technology (ERAST) program sponsored the Altus UAV in a successful measurement of atmospheric radiation over Kauai, Hawaii. In 2002, ERAST sponsored two missions; the solar-powered Pathfinder Plus UAV performed high resolution imaging of coffee fields in Kauai, and the Altus Cumulus Electrification Study (ACES) measured electric fields near lightning storms in Key West, Florida using the Altus UAV [Wegener and Schoenung, 2003]. More recently, imaging of uncontrolled forest fires in Alaska was performed from the Altair UAV [NASA, 2004; Wegerbauer, 2004].

This paper describes a system study of a water vapor DIAL system that could be implemented on an Altair UAV platform. This system would be used to map the concentration of water vapor from a height of 10,000 m to ground level. The system performance is evaluated with respect to mass, volume, and power. We also assess the potential for deployment of additional instrumentation to carry out simultaneous studies on the Altair and discuss critical challenges related to environmental stresses in the Altair payload compartment (e.g., temperature, humidity, and shock and vibration loading).

1.1 The DIAL Technique

Differential Absorption Lidar (DIAL) is used to measure chemical concentrations (such as ozone, water vapor, and pollutants) in the atmosphere. A DIAL system uses laser pulses at two different wavelengths and compares the scattered intensity of the signals to derive the water vapor concentration as a function of range. Figure 1 is a pictorial representation of the DIAL technique. A laser pulse is generated and emitted into the atmosphere. The laser pulses alternate between an absorbing (on-line) and non-absorbing (off-line) wavelength of the water vapor molecule in the atmosphere as shown in Figure 2. The laser radiation collides with airborne molecules and aerosols and undergoes absorption and scattering. A small portion of the on- and off-line radiation is backscattered toward a collecting telescope. The backscattered signal is digitized and this information is used in the DIAL equation to calculate the water vapor concentration as a function of range.

For the system discussed here, the "on"-line laser wavelength coincides with the 946.0003nm absorption line of the water vapor molecule; while the "off"-line laser wavelength is at a nearby wavelength (outside the absorption spectrum). The laser signals are emitted into the atmosphere where the light interacts with gases and particles in the atmosphere. Interactions with both laser signals result in backscattered photons. The back-scattered laser signal is attenuated by the inherent losses associated with propagation in the atmosphere. Specifically, the backscatter intensity falls off as the inverse square of the distance traveled ($1/d^2$, where d represents distance). Interactions with the "on"-line 946.0003nm laser signal results in a weaker backscattered signal due to the additional attenuation related to absorption by the water vapor molecules. The difference in intensity between the two return signals can be used to deduce the concentration of the water vapor as a function of range.

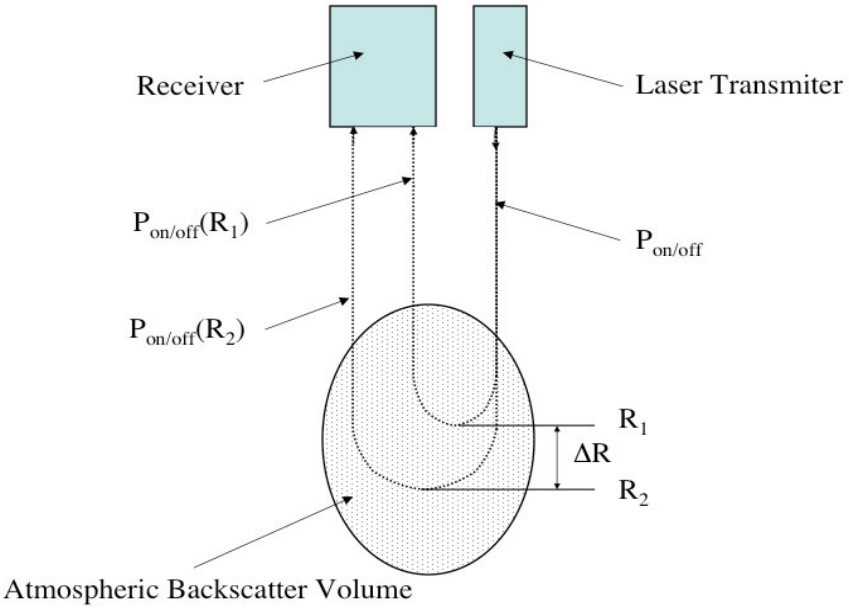

Figure 1. Fundamental processes in differential absorption lidar

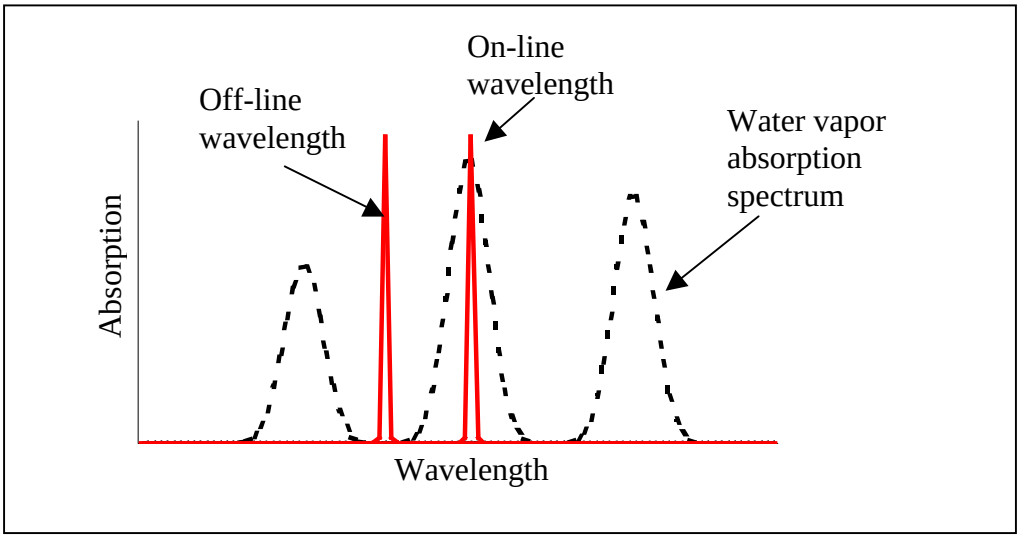

Figure 2. Pictorial representation of DIAL laser pulse spectrum and water vapor absorption spectrum

1.1.2 The DIAL Equation

The DIAL technique builds upon the principles of a conventional lidar system. The laser signal returned in a backscattered signal called the LIDAR equation is,

$$E(\lambda,R) = \frac{E_1 c\,\tau_d A_0\,\xi(\lambda)\,\zeta(R)\,\beta(\lambda,R)\,T^2(\lambda,R)}{2R^2} \qquad (1)$$

where,

$E(\lambda,R)$	backscattered energy received at the detector from laser wavelength λ at range R
E_1	output energy of transmitted laser pulse
$\xi(\lambda)$	spectral transmission factor of receiving system, including the impact of filters, mirrors, and other selecting optics
$\zeta(R)$	probability of radiation at range *R* reaching the receiver based on geometrical considerations
$\beta(\lambda,R)$	volume backscattering coefficient
$T(\lambda,R)$	atmospheric transmission factor over range *R*
A_0	cross-sectional area of receiver telescope (A_0/R^2 is acceptance angle of receiver optics, *R* is range from scattering molecule to receiver)
c	speed of light
τ_d	laser pulse width

DIAL is a measurement of the ratio of the backscattered on- and off-line power. Converting the LIDAR expression above (Eq. 1) to an expression in terms of power received where $P = E/\tau_L$ (τ_L is laser pulse width), results in the DIAL equation as,

$$\frac{(P_{on})_2(\lambda_{on},R)}{(P_{off})_2(\lambda_{off},R)} = \frac{(P_{on})_1\xi(\lambda_{on})\beta(\lambda_{on},R)T^2(\lambda_{on},R)}{(P_{off})_1\xi(\lambda_{off})\beta(\lambda_{off},R)T^2(\lambda_{off},R)} \qquad (2)$$

and the molecule concentration is,

$$N(R) = \frac{1}{2\Delta\sigma(R_2 - R_1)} \ln \left[\frac{P_{on}(R_1) P_{off}(R_2)}{P_{on}(R_2) P_{off}(R_1)} \right] \quad (3)$$

where,

$\Delta\sigma$ difference in absorption cross-section between on- and off-line wavelengths

$R_2 - R_1$ range cell over which the molecule concentration is calculated

The simplified expression compares the decay of on- and off-line signals in a defined range ($R_2 - R_1$), and it can be shown that the DIAL calculation is not affected by the pulse power of the laser source. Also, the smaller the range cell (R_2-R_1), the more accurate the calculation. For a more complete treatment of this derivation see Kovalov and Eichinger (2004).

1.2 Unmanned Aerial Vehicle (UAV) Platforms

NASA Langley is currently exploring the use of UAV platforms for lidar applications. Table 1 summarizes general characteristics of four commercially available UAV's: Altus II, Perseus B, Pathfinder-Plus, and Altair. These vehicles represent an existing infrastructure to support NASA Langley and other organizations involved in atmospheric research. The Altair has the largest payload and electrical power capacity and it has the longest flight endurance, allowing continuous data collection capabilities for periods of 32 hours. The maximum flight altitude of 15.2km exceeds the requirements for studies of the troposphere, and its 75 m/s airspeed is the second fastest of the UAV's listed.

Table 1. General Characteristics of UAV's

Characteristic	**Altus II (dual alternator)**	**Perseus B**	**Pathfinder-Plus**	**Altair**
Manufacturer	General Atomics	Aurora Flight Sciences	AeroVironment	General Atomics
Maximum Payload (kg)	150	80	45	300
Maximum Payload power (kW)	2-5	1.0	0.5 – 1	4.5
Payload volume (m^3)	0.733	0.7	N/A	1.56
Maximum Altitude (km)	20.0	20.0	24	15.2
Endurance (hr)	24 @ 10.7km	18.6 @ 20km	6.5 @ 18km	32 @ 15.2km
Takeoff Weight (kg)	907	1100	330	1588
Airspeed (m/s)	33 – 36	41 – 150	27	75

The Altair UAV, shown in Figure 3, is produced by General Atomics Aeronautical Systems, Incorporated. It is an extended-wing V-tail configured aircraft, resulting in long flight duration performance. The first successful flight of the Altair occurred in June, 2003 [NASA, 2003]. Isometric drawings of the Altair and additional mechanical and electrical characteristics have been obtained from the product catalog and are presented in Figure 4 and Table 2 [GAAS, 2001]. Additional information on the Altair UAV may be obtained from the General Atomics Aeronautical Systems website (www.uav.com).

The first order design considerations for this study include payload weight, volume, and power constraints. However, the final design must account for environmental requirements such as mechanical stress under take-off, landing, and in-flight conditions; temperature and humidity stresses in the payload compartment; data transfer and other communications protocols for remote operation of system components; center of gravity and allowable distribution of weight requirements; and mechanical requirements for attaching the lidar system to the aircraft.

Table 2. Mechanical and Environmental Performance Characteristics of Altair Payload Bay

Altair Performance Summary	
Parameter	**Performance**
Dive Speed (m/s)	115.2m/s (224 KIAS)
Maximum climb rate (m/s)	10.2m/s
Maximum range (km)	4790km
Payload compartment temperature	-55 C to +75 C
Humidity	100% humidity
Shock loading	10gs for 11 seconds ($98 m/s^2$)
Vibration loading	2g peak at 100Hz
Acceleration conditions – (design load limits)	-2.3g to +5.7g momentary; -1.5g to +3.8g sustained

Figure 3. View of Altair UAV at landing

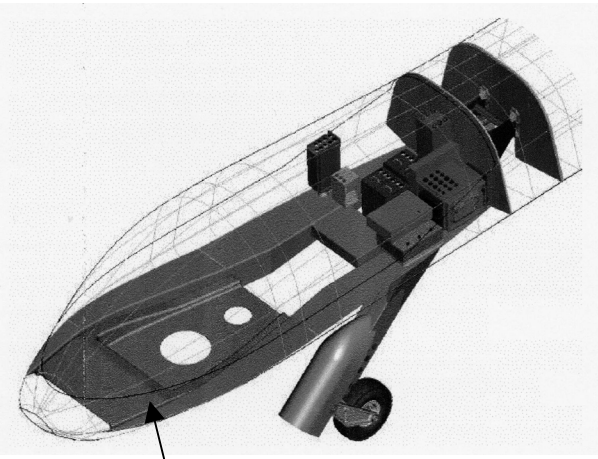

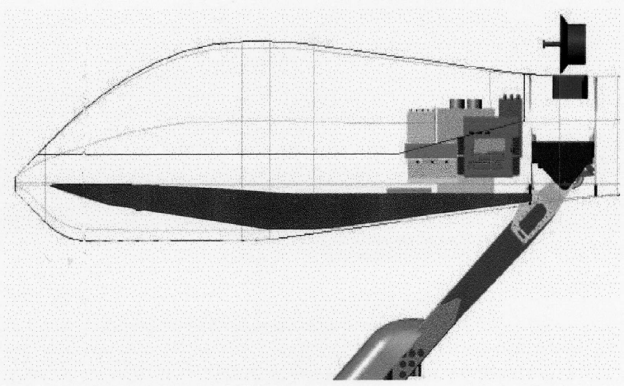

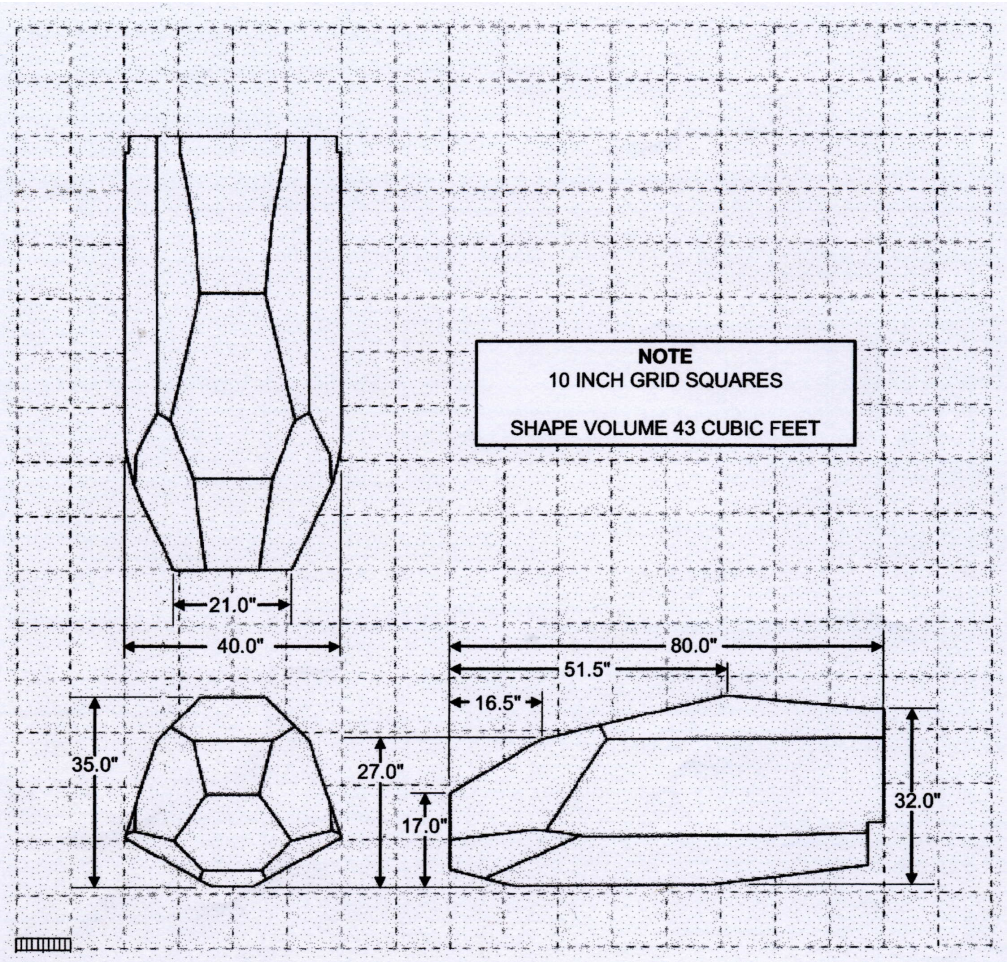

Note A: The customized mounting rail shown in this figure is not standard equipment for the Altair payload compartment. General Atomics will develop a unique design for each mission.

Figure 4. Isometric views of Altair payload compartment (left), and external dimensions of Altair payload compartment (right) [GAAS, 2001].

2. Water Vapor DIAL System

This section discusses system requirements for a water vapor DIAL system to be deployed on an Altair unmanned aerial vehicle. The presentation is organized into four general areas – Laser Generation, Receiver, Mounted DIAL System, and DIAL System Performance.

2.1 DIAL Laser Transmitter

The DIAL laser transmitter is chosen based on the absorption spectrum of the water vapor molecule. In our application, the DIAL system will be used to determine water vapor concentrations in the atmosphere at heights ranging from 0 to 10,000 meters, with a vertical resolution of 30 meters and a horizontal resolution of 150 meters.

Figure 5 shows the absorption spectrum for water vapor from 945.35 nm to 946.20 nm [DeYoung, 2004]. The absorption line at 946.0003 nm with 8.47 pm linewidth is chosen for our water vapor DIAL "on"-line wavelength. For this preliminary design, a laser source with tunable emission near 946 nm and a linewidth less than 1 pm is desired. The off-line laser signal should coincide with a spectral region where no absorption occurs, such as the region from 945.65 nm – 945.95 nm. Hence, a laser system with a tuning range from 945.5 nm to 946.1 nm would meet our "on" and "off"-line water vapor DIAL laser requirements. Q-switched Nd:YAG/Cr^{+4}:YAG solid state lasers with emission at 946 nm have been demonstrated [Liu et al, 1997]. The Ultrarad, Incorporated RL05-946 Nd:YAG microchip laser is a commercially available version of the Q-switched Nd:YAG/Cr^{+4}:YAG microchip laser (see www.ruslaser.com). The RL05-946 emits at 946 nm and produces pulsed output powers to 300μJ at 1 kHz repetition rates. However, the RL05-946 is not wavelength stabilized and the linewidth does not meet our requirements. To achieve the necessary wavelength stability an injection locking approach is adopted. A schematic of the injection-locked water vapor DIAL laser transmitter is presented in Figure 6. Figure 7 presents a photographed image of the RL05-946 laser head.

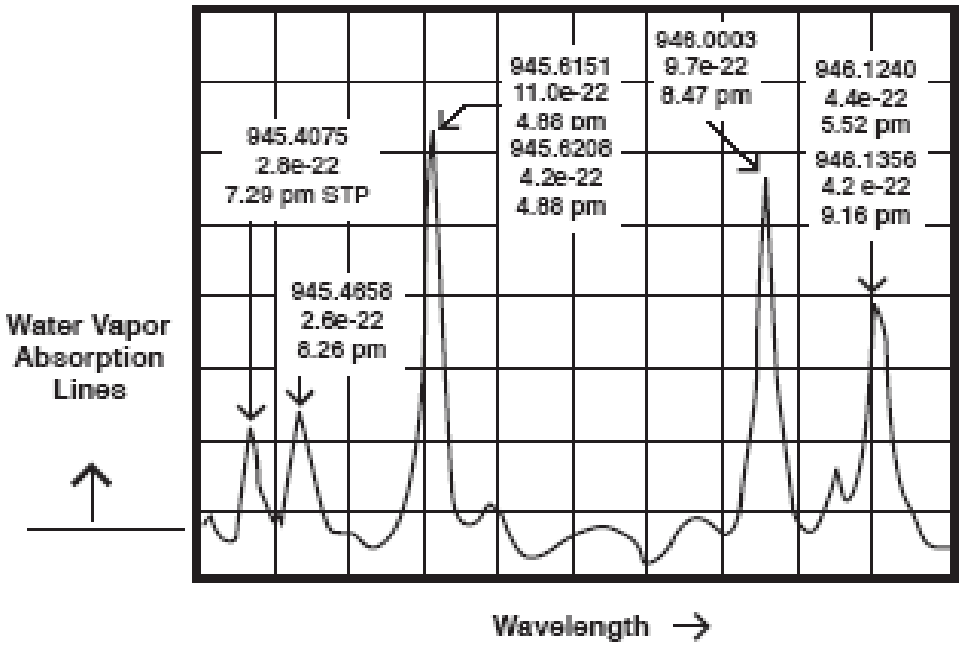

Figure 5. Water vapor absorption spectrum

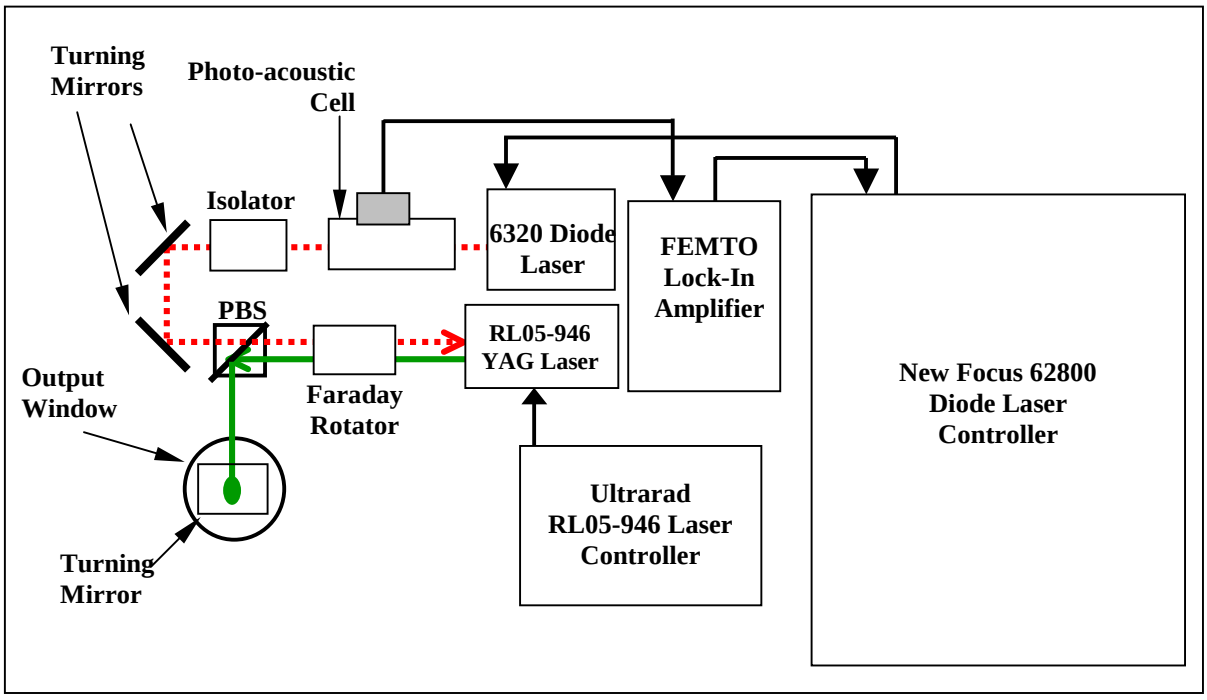

Figure 6. Schematic for water vapor DIAL laser transmitter

Figure 7. Ultrarad, Incorporated RL05-946 Nd:YAG microchip laser

2.1.1 Laser Pulse Width and Repetition Frequency

DIAL measurements are vertically resolution limited by the sample rate at which the backscattered signal is captured. For the case of 30 m vertical resolution, capture events would take place at intervals of 0.200μs (or 30 m). This corresponds to a capture rate at the receiver of 5MHz. The sample rate is helpful in determining the laser pulse width, which should be much less than the sample period of 0.200μs.

We wish to profile the water vapor concentration from approximately 10 km down to ground level. The maximum laser pulse repetition frequency is determined from the flight altitude of the UAV. Assuming a flight altitude of 12 km, the laser signal must travel a total of 24 km to reach the ground and return to the receiver. Thus, the roundtrip transit time is 80μs, corresponding to a maximum repetition rate of 12.5kHz. The RL05-946 laser to be used in our water vapor DIAL laser transmitter has a repetition rate of 1KHz, which is much less than the maximum repetition rate.

In our system study, we assume that signal averaging will typically occur over a period of 2 sec. Since the Altair UAV travels no faster than 75 m/s, the horizontal resolution for our measurements will be 150 m. During this time, 2,000 water vapor profiles will be captured and averaged together to produce a water vapor profile as a function of range.

The on-line laser wavelength must be locked to the 946.0003 nm water vapor absorption line, and the laser linewidth must also be much less than the absorption linewidth. A novel locking technique that uses a photo-acoustic cell containing a water vapor sample placed in the path of the laser source is used to stabilize the laser wavelength [Varanasi et al, 2001]. The cell creates an acoustic signal that is proportional to the absorption within the cell; the greater the absorption, the stronger the acoustic signal. A microphone is attached to the cell and a feedback signal from the microphone is used to tune the laser wavelength to the peak of the 946.0003 nm absorption line.

An injection locking technique is used to achieve narrow line laser output for the on-line wavelength. A New Focus 6320 tunable diode seed laser is current tuned by a sinusoidal dither signal coupled with the feedback signal from the photo-acoustic cell. The dither current alternately tunes the seed laser output to match the on-line, then off-line wavelength of the water vapor cell. The seed laser radiation is injected into the Ultarad RL05-946 laser, which follows the seed laser wavelength through the injection locking process. Table 3 outlines the optical requirements for the water vapor DIAL laser transmitter.

Table 3. DIAL Laser Transmitter Requirements

Parameter	Specification	Comment
Wavelength	946nm “on”-line output, tunable range from 945.5nm to 946.1nm	Matches absorption region for water vapor
Linewidth	FWHM <1 pm	Less than 20% of 8.47pm absorption linewidth
Pulse Energy	300μJ per pulse	Output energy requirement for on- and off-line emission
Pulse width and repetition frequency	75 ns pulse width at 1kHz pulse repetition frequency	

2.1.4 DIAL Laser Transmitter Design

A full schematic of the DIAL laser transmitter design is presented in Figure 6. The figure illustrates an injection locked Ultrarad, Incorporated Nd:YAG/Cr^{+4}:YAG[1] laser. The locking laser is a New Focus model 6320 tunable diode laser. The diode laser is temperature stabilized and is tuned using a feedback signal from the photo-acoustic cell and lock-in amplifier. The schematic also shows isolation stages at the output of the seed laser diode and the Nd:YAG laser to prevent back-reflections into the seed laser cavity from the Nd:YAG laser, windows, or other components in the beam path. Finally, beam splitters

[1] The Nd:YAG/Cr^{+4}:YAG laser will be referred to as a Nd:YAG laser.

and turning mirrors are used to steer the beam toward the output window of the aircraft. The steering design requires linearly polarized output from the seed laser diode and the Nd:YAG laser. A list of commercially available components that meet the design requirements of the DIAL laser design is presented in Table 4.

Table 4. DIAL Laser Transmitter Parts List

Part	Manufacturer	Part Number	Specifications
Nd:YAG Laser and laser controller unit	Ultrarad, Incorporated	RL05-946	YAG:Nd/YAG:Cr^{+4} 946 nm emission 1 kHz repetition frequency M^2 >1.2[2] (see footnote) 1.5 – 2 ns pulse width
Tunable Diode Laser	New Focus, Incorporated	TLB-6320	960 – 994 nm (special order or alternate vendor is necessary) FWHM < 1pm 100 MHz modulation bandwidth
Photo-acoustic Absorption Cell	In-house design, NASA Langley Research Center		
Lock-In Amplifier	FEMTO	LIA-MV-150	10Hz – 45KHz frequency Digital Phase Shifter
Optical Isolator	Electro-Optics Technology	LD381980	> 30dB isolation 960 - 1000nm 90% transmission 3x8mm clear aperture
Faraday Rotator	Electro-Optics Technology	LD38R980	> 98% transmission 960 – 1000nm > 30 dB isolation 3x9mm clear aperture
Polarizing Beamsplitter	New Focus, Incorporated	Model 5812	500:1 Extinction ratio for 650 – 1000nm

2.2. DIAL Receiver System

The DIAL receiver system includes a collecting telescope, a photo-detection module, and a computer to digitize, store and process the water vapor profiles. A Newtonian telescope assembly, as shown in Figure 8, is used to capture and focus the backscattered light into a large core optical fiber. The telescope assembly includes a 16″ diameter parabolic mirror to collect and focus the back-scattered light, and the optical fiber is mounted to a translational stage to optimize the telescope capture efficiency. A theoretical review of the expected efficiency is given in Shah (2003) and Stenholm and DeYoung (2001). The parabolic mirror is mounted inside a 16″ diameter carbon-fiber-epoxy tube just inside the entry window of the UAV.

[2] M^2, the beam quality, is a figure of merit to characterize the actual beam divergence in comparison to a diffraction limited TEM_{00} beam. A TEM_{00} beam would have an M^2 of 1.0.

The fiber cable carries the collected light to a photo-detecting unit as shown in Figure 9. The photo-detecting unit includes an Avalanche Photo-Diode (APD) to capture the intense near field return signals, and a Single Photon Counting Module (SPCM) with amplifier for weaker far-field return signals. The APD and SPCM convert the received optical signal into an electronic signal that can be digitized and stored by an on-board computer. Table 5 presents the DIAL receiver parts list.

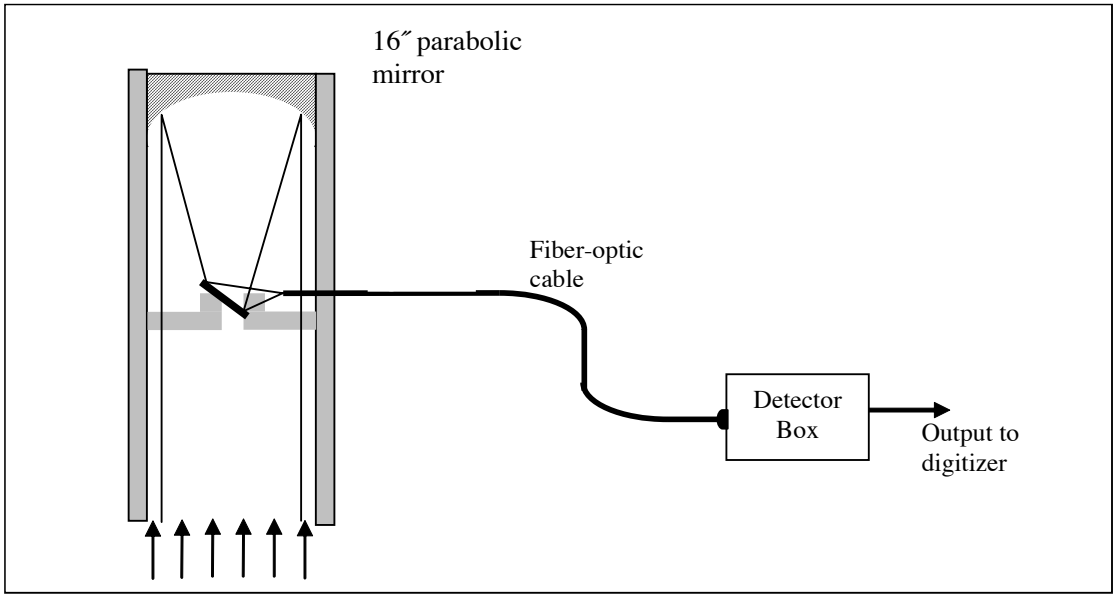

Figure 8. Newtonian telescope with fiber-coupled output signal

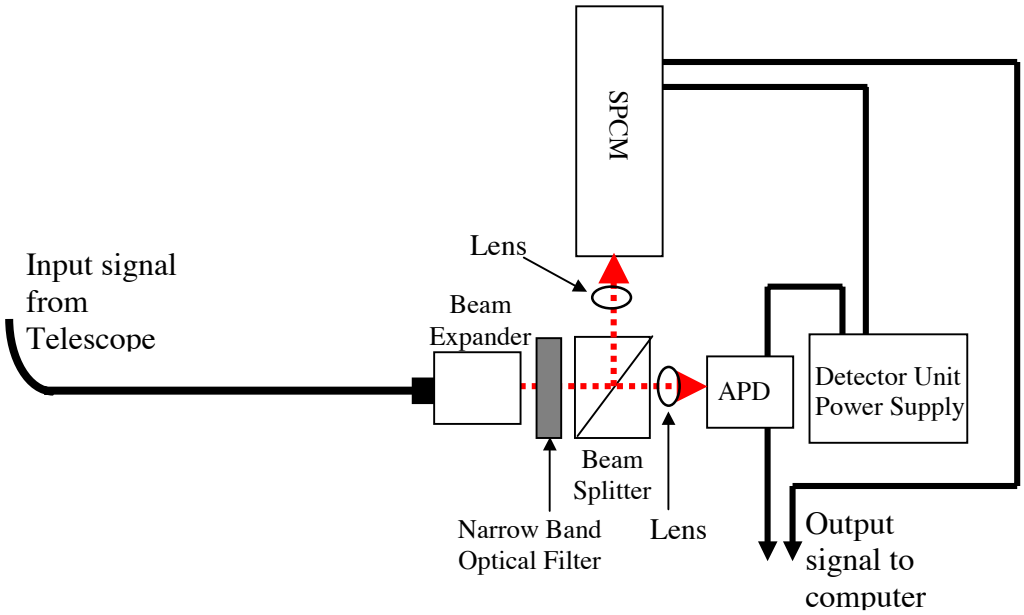

Figure 9. Photo-detection unit

Table 5. List of Components for Water Vapor DIAL Receiver System

Part	Manufacturer	Part Number	Specifications
Parabolic Mirror	Stablite, Inc.	Custom order	355mm (16") diam. , 610mm (24") radius of curvature; HR coat for 946nm > 99% reflecting
Avalanche Photodiode	Advanced Photonix	118-70-72-661	3-mm diam. APD module with TE cooler and transimpedance amplifier
Single Photon Counting Module	Perkin-Elmer	SPCM-ARQ-21	
Narrow Band Filter	CVI Laser, Inc.	F10-950.0-4	Center Wavelength: 946nm FWHM: 10nm
Beam Splitter	Melles Griot	PCB-980-80-050-UNP	Non-polarizing cube beam-splitter 12.5mm edge dimension 80/20 reflecting ratio at 980nm
Focusing Lens	Melles Griot	01-LAG-001	Plano-Convex Condensing Aspherical Lens; 15mm diam.; 12mm focal length; AR V-coat at 946nm
Fiber Optic Cable	Thor Labs	AFS-105.125Y	105μm diam. core optical fiber NA 0.25; 125 μm clad diam.; 250 μm jacket diam.

3. Lidar System Mounted in Altair UAV

Figure 10 shows the DIAL laser and receiver components mounted onto a carbon-fiber-epoxy breadboard. The breadboard features an aluminum honeycomb with carbon-epoxy exterior. An on-board computer is mounted onto the bottom of the breadboard as shown in Figure 11. A cover is provided for the DIAL laser, receiver, and computer to provide moisture protection and thermal stability for the electronic and optical components. The breadboard assembly is then mounted into the Altair payload compartment and affixed to a custom designed mounting rail (not shown in Figures 10 and 11; see Altair designer handbook). The mounting rail design is generated through discussions with the Altair manufacturer, General Atomics Aeronautical Systems. Figure 4 shows an example mounting rail design that has been developed for another research mission.

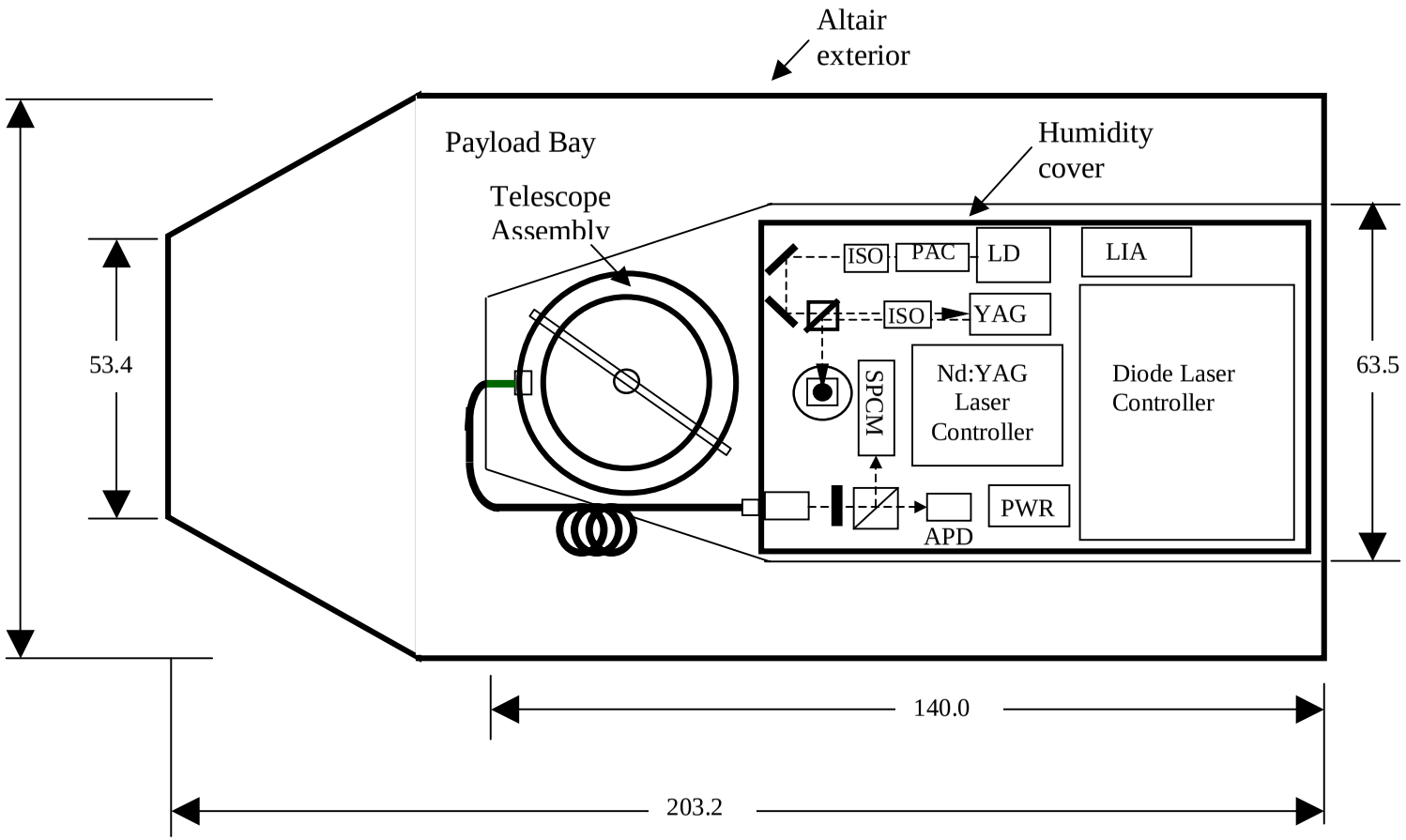

Figure 10. Top view of water vapor DIAL system mounted in Altair payload compartment (scaled drawing with dimensions in cm). ISO – isolator; PAC – photo-acoustic cell; LD- laser diode; LIA- lock-in amplifier; YAG- Ultrarad Nd:YAG laser head; SPCM – single photon counting module; APD – Avalanche photodiode; PWR – detector power supply

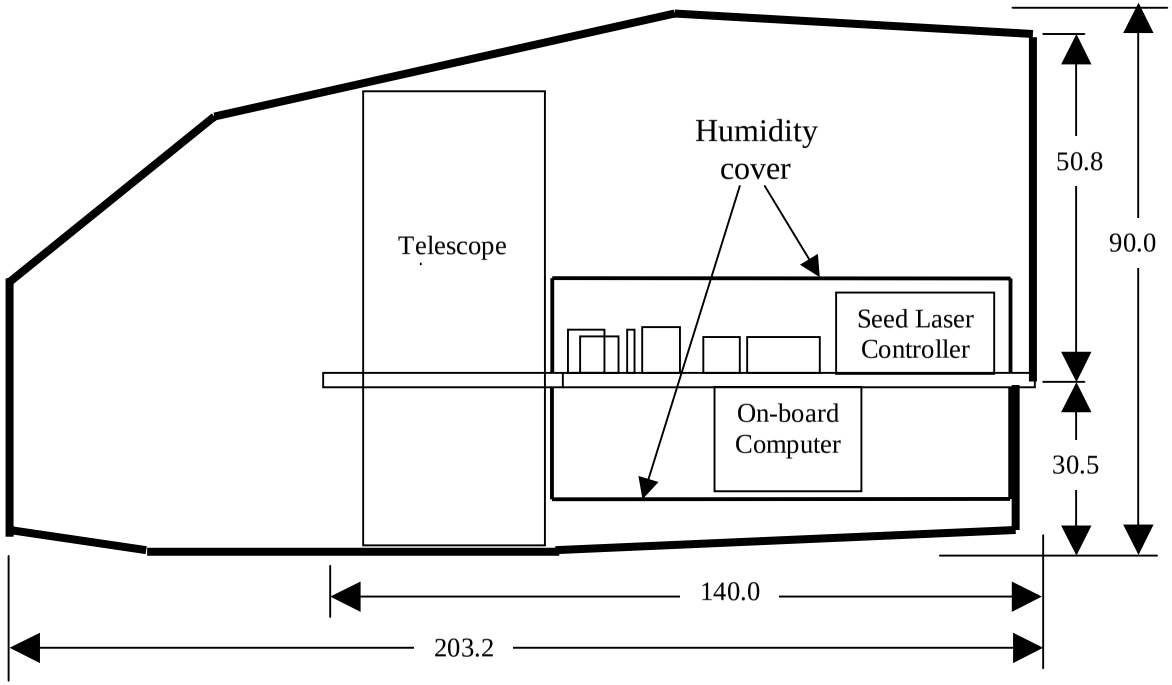

Figure 11. Side view of water vapor DIAL system mounted in Altair payload compartment (scaled drawing with dimensions in cm).

4. DIAL System Performance

Table 6 presents a catalog of the DIAL components and their respective mass, volume, and electrical power requirements. The total volume, mass, and electrical requirements and a comparison to the Altair UAV payload capacity are listed at the bottom of the table. The results show that the proposed water vapor DIAL system design will consume 19% of the payload volume, 18% of the payload weight capacity, and 16 % of the available power. The preliminary water vapor DIAL system design performance is acceptable in all of the critical categories for this study. The current design also provides an opportunity to support multiple UAV users on simultaneously executed missions, thereby reducing individual costs.

Although the water vapor system design is well within the Altair capabilities, there are several additional requirements that a successful design must address. In particular, temperature, humidity, and mechanical shock loading are severe and should be accounted for in the system design. Table 2 (above) lists the mechanical and environmental conditions that would exist in the Altair payload compartment during takeoff, landing, and under in-flight conditions.

The payload compartment temperature will range from temperatures as high as 75º C at takeoff, down to -60º C during the flight. These temperatures have been derived based on manufacturer suggested external air conditions. The in-flight temperature is most significant since this is the condition under which the water vapor DIAL system will operate. It is generally found that cold is good for electronic noise and the elimination of thermally activated failure mechanisms. However, cold temperatures can cause mechanical failure or misalignment of the optoelectronic components. Cold temperatures promote condensation, and some components will require active temperature control. Possible solutions include the application of thermal barriers in critical locations, implementing active heating strategies, requiring hermitic seals for key components, or using more robust encapsulating or adhesive materials.

A series of performance tests under payload temperature conditions should be executed to insure that the DIAL laser emitter assembly and other system components will operate as required under the extreme cold temperature conditions of the Altair payload compartment. The tests should include a temperature cycle up to the maximum payload compartment temperature of 75º C, and a temperature dwell at -60º C. The tests should also apply humidity and mechanical shock and vibration stresses that reflect in-flight and landing conditions for the Altair payload bay. The test period should be long enough to allow all system components to reach temperature equilibrium.

Table 6. Catalog of DIAL System Component Mass, Volume, and Electrical Requirements

Part	Manufacturer	Part Number	Vol. (m^3)	Mass (kg)	Power (kW)
Tunable Diode Laser and Controller	New Focus	6320 Tunable Diode Laser	neglect	1.36	0.100
		62800 Diode Laser Controller	neglect	11.79	
Nd:YAG Laser and Controller	Ultrarad, Incorporated	RL05-946 Laser	neglect	1.0	0.100
		RL05 Laser Controller	neglect		
Lock-In Amplifier	FEMTO	LIA-MV-150	neglect	0.37	negligible
Parabolic Mirror + Tube Mount	Assembled in-house		9.30e-2	7.48	N/A
Avalanche Photodiode	Advanced Photonix	118-70-72-661	neglect	2.2	See APD/SPCM power supply
Single Photon Counting Module	Perkin-Elmer	SPCM-ARQ-21	neglect		See APD/SPCM power supply
Narrow Band Filter	CVI Laser, Inc.	F10-950.0-4	neglect		N/A
Beam Expander	Melles Griot		neglect		N/A
Beam Splitter	Melles Griot	PCB-980-80-050-UNP	neglect		N/A
Focusing Lenses	Melles Griot	01-LAG-001	neglect		N/A
APD/SPCM Power Supply	Assembled in-house		neglect	3.18	negligible
On-board Computer	Assembled in-house		neglect	11.34	0.30
Photo-acoustic Cell w/ microphone	Assembled in-house		neglect	<2.0	negligible
Optical Isolator	Electro-Optics Tech.	LD381980	neglect		N/A
Faraday Rotator	Electro-Optics Tech.	LD38R980	neglect		N/A
Polarizing Beam-splitter (PBS)	New Focus, Incorporated	Model 5812	neglect		N/A
Fiber Optic Cable	Thor Labs	AFS-105.125Y	N/A	N/A	N/A
Breadboard	carbon-fiber-epoxy w/alum. fill		4.12e-2	7.48	N/A
Miscellaneous	cabling, hardware, optical mounts, etc.		neglect	2.5	N/A
Humidity cover with gasket	In-house assembly (approx. weight 10lbs.)	35" x 25" x 6" (top); 20" x 25" x 8" (bot.)	*1.52e-1	4.53	N/A
Clear window seal for telescope	JML Optics	Special order – 16" diameter fused silica window	N/A	4.53	N/A
TOTAL (w/ seal)	**Absolute values**		**2.89e-1**	**52.26**	**5.08e-1**
	% Altair capacity		**18.5**	**17.4**	**11.3**

*Note: Humidity cover volume replaces volume for all parts except breadboard and telescope

The mechanical shock and vibration characteristics for the Altair payload are listed in Table 2 (above). These conditions should be replicated when testing under operating conditions activities are performed. Dynamic modeling of the breadboard design should be performed to insure that the characteristic vibration frequencies for the Altair payload are not matched to resonant frequencies of the board design. If mode matching occurs, the board will experience severe mechanical stress and board cracking or fracture may result. Board dampeners may be used to eliminate mode matching [Pecht, 1991].

Due to the extreme humidity conditions within the Altair payload compartment, a sealed cover unit for the top and bottom side of the water vapor DIAL system is recommended as shown in Figure 10. A window to seal the Newtonian telescope tube is also recommended. The sealed compartments should be flooded with nitrogen gas at the start of each mission, or a desiccant material should be placed inside the compartments to remove moisture from the enclosed air**.**

5. Suggested Improvements

The proposed water vapor DIAL system design is well within the payload capacity of the Altair UAV. The design also includes special features to account for mechanical and environmental stresses of the aircraft. However, the design has not been optimized for the primary performance parameters; weight, volume, and power. One area for which an immediate improvement can be realized is through the use of customized electronic units. The lock-in amplifier unit could be replaced by a customized computer card. The current lock-in amplifier unit is located on the top side of the current breadboard design arrangement. This module could be replaced by a printed circuit board (PCB) assembly. The PCB would be installed in an expansion slot of the computer assembly. The switch would free up a 51mm x 157mm footprint on the breadboard, and the weight improvement would be 270 gr. Table 7 lists a commercially available lock-in amplifier PCB that meets the design requirements for the water vapor DIAL system.

A second area that could be explored is the use of advanced fiber-optic products to replace passive optical components in the water vapor DIAL receiver unit. Advances in fiber optic technology could be applied to several of the front-end optical components in the water vapor DIAL receiver unit. Advanced fiber-optic products could be used to replace the beam expander, narrow band filter and beam-splitter. Stenholm (2001) has done a study demonstrating a water vapor DIAL receiver with a fiber optic narrow band filter. The Stenholm approach employed a single-mode fiber with Bragg gratings for the on- and off-line signals. However, Zhao (2000) and Pasupathy (2000) have demonstrated Bragg grating filters in multimode fibers with acceptable filtering performance. A series of experiments to identify the most

suitable approach for the water vapor DIAL receiver using multimode fibers is suggested. Once an appropriate filtering approach is identified, the filter may be linked to a 2x2 (dual input/dual output) fiber optic coupler to achieve an appropriate splitting ratio between fiber pigtailed versions of the APD and SPCM units. The ratio of light energy entering the APD and SPCM can take on any value and is controlled by the coupler design. Replacing the beam expander, narrow band filter, and beamsplitter with fiber products will free an area of approximately 105 cm^2 on the breadboard (16.5 x 6.35 cm footprint), and the weight improvement is estimated to be near 1kg.

One concern that will require further study related to the use of fiber optic products is the impact of mechanical and temperature stress on performance. For example, the extreme temperature cycling in the Altair UAV payload compartment may result in large variability in fiber grating performance, as well as the performance of encapsulant or adhesive materials that may be used to maintain alignment. The mechanical shock and vibration environment may also degrade the grating performance, as well as to disrupt or degrade the fiber alignment. Table 7 presents a list of commercially available fiber optic components that meet the requirements of the water vapor DIAL system.

Table 7. Optimized Water Vapor DIAL Design Parts List

Part	Manufacturer	Part Number	Volume Reduction (m^3)	Footprint Reduction (cm)	Weight Reduction (kg)
Lock-In Amplifier PCB	FEMTO	LIA-BV-150-H	2.16e-4	5.1 x 15.7	.270
Fiber Optic Cable Graded Index (GRIN) Lens Collimator	Thor Labs	F220SMA-B	5.33e-4	16.5 x 6.35	<1.0
Fiber Optic 2x2 Coupler	Thor Labs	FC-980-90-FC			
Fiber Optic Narrow Line Filter	Oz Optics or in-house	Special order: 3nm FWHM @ 946nm; multimode fiber			

In addition to the above outlined modifications, an alternative laser transmitter design is proposed. Tunable dual-frequency lasers have been demonstrated using the birefringent properties in solid-state lasers [Gudelev et al, 2003]. The dual-orthogonal modes are produced within a single laser cavity when birefringent materials are located in the beam path. The frequency difference between the orthogonal modes can be tuned by controlling the degree of birefringence through mechanical stress or temperature tuning. These same parameters can also be used to stabilize the absolute wavelength of a laser mode. We introduce here a novel design that will lock the *s*- mode of a Nd:YAG/Cr:YAG laser to the 946 nm water vapor absorption line, and tune the *p*- mode to a wavelength that is 0.5 – 0.7nm away from the *s*- mode, thus producing the on- and off-line emission needed for a DIAL laser transmitter.

The proposed Q-switched dual-orthogonal-mode Nd:YAG/Cr:YAG laser is shown in Figure 12. The laser cavity includes a calcite crystal to achieve spatial separation of the orthogonal modes inside the laser gain medium, a piezo-tunable birefringent material to achieve coarse tuning of the frequency difference between the orthogonal modes, and piezo tuning of the laser crystal for fine tuning. Some of the challenges must be addressed for the dual-orthogonal-mode laser include the elimination of multi-longitudinal mode operation due to spatial hole burning, and determining an acceptable approach for achieving a Q-switched pulse width of 50-100ns. Differential lasing thresholds for the orthogonal modes may occur in the proposed configuration. Finally, developing a suitable feedback mechanism to achieve fine and coarse tuning, while also maintaining a lock to the 946nm water vapor absorption line may also be problematic. A series of proof of concept experiments to test for reasonable tuning with a 100's of nanosecond range Q-switched output is suggested. The proposed dual-orthogonal-mode laser would replace the tunable diode laser and Nd:YAG microchip laser in the current design. In the present design, the tunable diode laser and controller account for 25.2% (13.15 kg) of the total weight for the water vapor DIAL system. It is believed that the dual-orthogonal-mode laser would be comparable in weight and size to the RL05-946 laser.

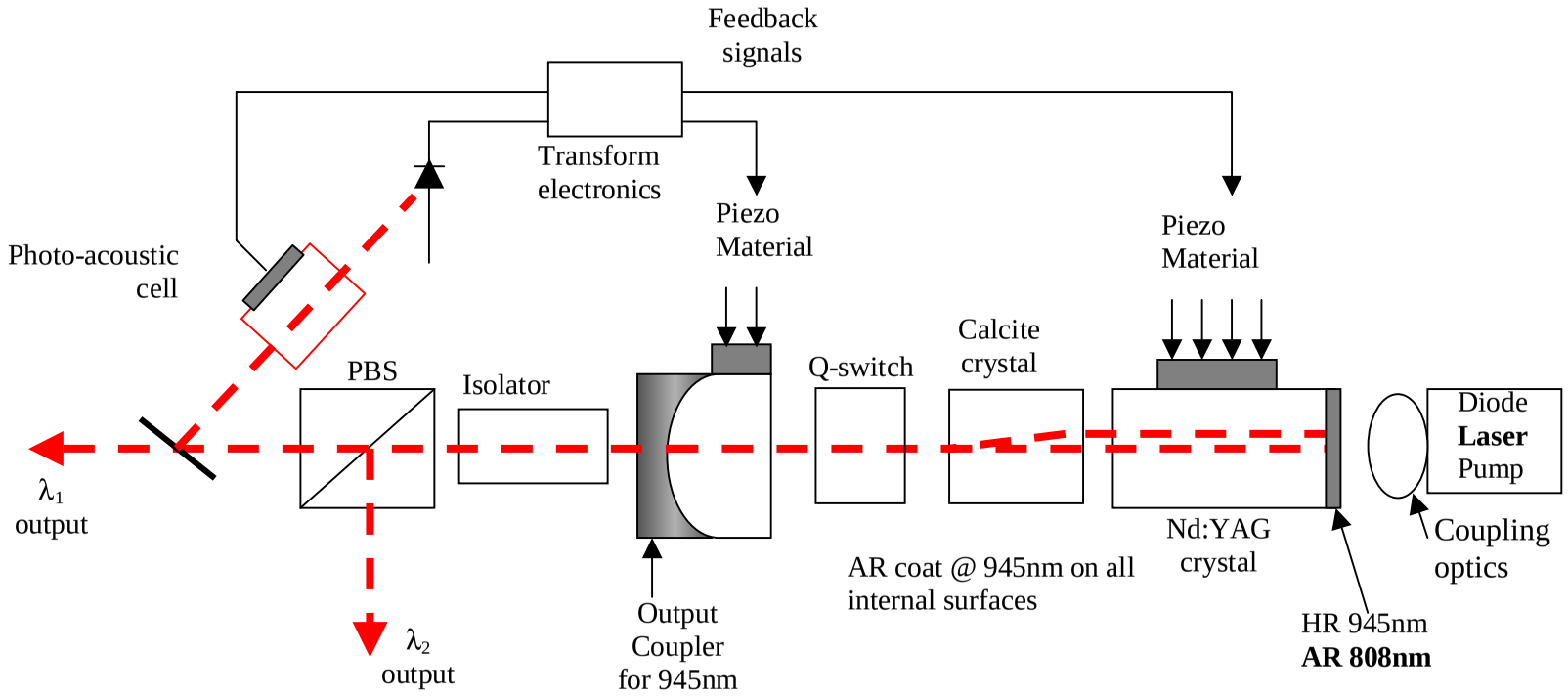

Design Features

- Wavelength separation is controlled by stress birefringence in laser crystal and output coupler
- Calcite crystal provides spatial separation of orthogonal modes (eliminates mode competition)
- Feedback from photo-acoustic cell can be used to lock laser output to desired wavelength

Challenges

- Multi-longitudinal mode lasing due to spatial hole burning
- Differential lasing threshold between orthogonal modes
- Increase tuning range from 70 to 200pm
- Q-switched output 50 – 100 ns pulse width
- Feedback circuit

Figure 12. Dual Orthogonal Mode Laser Design

6. Conclusions

A preliminary system study for a water vapor DIAL system deployed on the Altair UAV has been presented. The design features commercially available laser transmitter components, including an injection-locked Nd:YAG microchip laser transmitter and a tunable diode laser to line narrow and lock the Nd:YAG laser to the 946.0003 nm water vapor absorption line. The DIAL receiver unit features a fiber-coupled Newtonian telescope, and commercially available avalanche photodiode and single photon counting module units. All components may be remotely controlled through an IEEE databus. The system also features hermetic sealing to prevent moisture-induced damage or degraded system performance. Pending the results of a dynamic modeling study to determine the weight distribution and center of gravity performance of a final design, the composite system is estimated to use approximately 19% of the available payload volume, 18% of the available payload weight, and 16% of the available power for payload components. The actual performance may vary depending upon modifications that may be required following the dynamic modeling study. Due to the extreme mechanical and environmental stresses inside the Altair UAV payload compartment, testing to identify probable failure modes is suggested. Alternative upgrades that would produce measurable weight and volume improvements include the use of customized electronic components and replacement of passive bulk optical components with fiber optic components. Finally, a novel dual-orthogonal-mode Nd:YAG laser design that has promise as a compact water vapor DIAL laser source is proposed.

References

Cohn, C. and C. Harper. 2004. Failure Free Integrated Circuit Packages. New York, NY: The McGraw-Hill Company.

DeYoung, R. J. Private communication, August 13, 2004.

GAAS (General Atomics Aeronautical Systems, Inc.). 2001. Altair Experimenter's Handbook. San Diego, CA: Aeronautical Systems.

Goldschmidt, S. and DeYoung, R.J. 1999. An Ozone Differential Absorption Lidar (DIAL) Receiver System for Use on Unpiloted Atmospheric Vehicles. NASA/TM-1999-209716. Hampton, VA: NASA Langley Research Center.

Ismail, S. and E. Browell. Airborne and Spaceborne Lidar Measurements of Water Vapor Profiles: A Sensitivity Analysis. Applied Opt., vol. 28, no. 17, Sept. 1, 1989, pp. 3603-3615.

Jursa, Adolph S., Sci. Ed.: Handbook of Geophysics and the Space Environment. Air Force Geophys. Lab., U.S. Air Force, 1985.

Kovalev, V. A., Eichinger, W. E. (2004). Elastic Lidar: Theory, Practice, and Analyses Methods. Hoboken, N.J.: John Wiley & Sons.

Machol, Janet L. et al. Preliminary Measurements with an Automated Compact Differential Absorption Lidar for the Profiling of Water Vapor. Applied Optics. Vol 43, No. 15, 20 May, 2004. pp. 3110 – 3121.

NIST (National Institute of Standards and Technology). Performance Analysis of Next-Generation LADAR for Manufacturing, Construction, and Mobility. Publication of United States Department of Commerce Technology Administration: National Institute of Standards and Technology. Washington, D.C: May 2004.

Parker, R. 2002. The Predator's War: UAVs Take Center Stage in War on Terrorism. Airman Magazine. December 2002. Viewable online at http://www.af.mil/news/airman/1202/aerial.html.

Pasupathy, V., Szkopek, T., Smith, P.W.E. 2000. Novel Multimode Fiber for Narrowband Bragg Grating Response. Optical Society of America. OCIS:060.2270.050.2770.

Pecht, M., 1991, Handbook of Electronic Packaging Design, Marcel Dekker, N. Y.

Shah, A.M. 2003. Atmospheric Water Vapor Lidar Measurements Using Analog Photon Counting Techniques. Master of Science Thesis, Old Dominion University, Norfolk, VA, August 2003.

Stenholm, I. And DeYoung, R.J. 2001. Ultra Narrowband Optical Filters for Water Vapor Differential Absorption Lidar (DIAL) Atmospheric Measurements. NASA/TM-2001-211261. Hampton, VA: NASA Langley Research Center.

Varanasi, P., Ranganayakamma, B., Mathur, S., Refaat, T., and C.R. Prasad. 2001. Measurement of the Absorption Characteristics of Water Vapor Saturation. Eleventh ARM Science Team Meeting Proceedings. Atlanta, Georgia. March 2001.

Wegener, S. and Schoenung, S. 2003. Lessons Learned from NASA UAV Science Demonstration Program Missions. Viewable online at: http://geo.arc.nasa.gov.

Wegerbauer, C. 2004. Mariner Deploys to Alaska. Press release of the General Atomics Aeronautical Systems, Incorporated. Farnborough, United Kingdom. July 19, 2004. Viewable online at: www.uav.com.

Zhao, W. and Claus, R.O. 2000. Optical fiber grating sensors in multimode fibers. Smart Mater. Struct. **9** (2000) 212-214.

REPORT DOCUMENTATION PAGE

Form Approved
OMB No. 0704-0188

1. REPORT DATE *(DD-MM-YYYY)*	2. REPORT TYPE	3. DATES COVERED *(From - To)*
01- 12 - 2004	Technical Memorandum	

4. TITLE AND SUBTITLE

A Water Vapor Differential Absorption LIDAR Design for Unpiloted Aerial Vehicles

5a. CONTRACT NUMBER

5b. GRANT NUMBER

5c. PROGRAM ELEMENT NUMBER

6. AUTHOR(S)

Mead, Patricia F.; and DeYoung, Russell J.

5d. PROJECT NUMBER

5e. TASK NUMBER

5f. WORK UNIT NUMBER

23-622-29-26

7. PERFORMING ORGANIZATION NAME(S) AND ADDRESS(ES)

NASA Langley Research Center
Hampton, VA 23681-2199

8. PERFORMING ORGANIZATION REPORT NUMBER

L-19063

9. SPONSORING/MONITORING AGENCY NAME(S) AND ADDRESS(ES)

National Aeronautics and Space Administration
Washington, DC 20546-0001

10. SPONSOR/MONITOR'S ACRONYM(S)

NASA

11. SPONSOR/MONITOR'S REPORT NUMBER(S)

NASA/TM-2004-213507

12. DISTRIBUTION/AVAILABILITY STATEMENT

Unclassified - Unlimited
Subject Category 35
Availability: NASA CASI (301) 621-0390

13. SUPPLEMENTARY NOTES

Mead: Norfolk State University; Deyoung: Langley Research Center
An electronic version can be found at http://techreports.larc.nasa.gov/ltrs/ or http://ntrs.nasa.gov

14. ABSTRACT

This system study proposes the deployment of a water vapor Differential Absorption LIDAR (DIAL) system on an Altair unmanned aerial vehicle (UAV) platform. The Altair offers improved payload weight and volume performance, and longer total flight time as compared to other commercial UAV's. This study has generated a preliminary design for an Altair based water vapor DIAL system. The design includes a proposed DIAL schematic, a review of mechanical challenges such as temperature and humidity stresses on UAV deployed DIAL systems, an assessment of the available capacity for additional instrumentation (based on the proposed design), and an overview of possible weight and volume improvements associated with the use of customized electronic and computer hardware, and through the integration of advanced fiber-optic and laser products. The results of the study show that less than 17% of the available weight, less than 19% of the volume capacity, and approximately 11% of the electrical capacity is utilized by the proposed water vapor DIAL system on the Altair UAV.

15. SUBJECT TERMS

Water vapor LIDAR; UAV instruments; LIDAR; DIAL

16. SECURITY CLASSIFICATION OF:			17. LIMITATION OF ABSTRACT	18. NUMBER OF PAGES	19a. NAME OF RESPONSIBLE PERSON
a. REPORT	b. ABSTRACT	c. THIS PAGE			STI Help Desk (email: help@sti.nasa.gov)
					19b. TELEPHONE NUMBER *(Include area code)*
U	U	U	UU	31	(301) 621-0390